Eur. Phys. J. B **46**, 301–308 (2005)
DOI: 10.1140/epjb/e2005-00253-9

THE EUROPEAN PHYSICAL JOURNAL B

Positive and negative refraction of magnetoinductive waves in two dimensions

R.R.A. Syms[1,a], E. Shamonina[2], and L. Solymar[1]

[1] Optical and Semiconductor Devices Group, Department of Electrical and Electronic Engineering, Imperial College London, Exhibition Road, London SW7 2AZ, UK
[2] Department of Physics, University of Osnabrück, 49069 Osnabrück, Germany

Received 12 April 2005
Published online 11 August 2005 –

Abstract. Previous studies of magnetoinductive waves in homogeneous media with resonant elements consisting of capacitively loaded metallic loops are extended to the case when a single wave from one medium is incident upon another one. The relationship between the input and output angles and the reflection and transmission coefficients are determined with the aid of the dispersion equation for different scenarios. An expression is obtained for the power density vector, and it is shown that its component perpendicular to the boundary is conserved across the boundary. Using different configurations of the elements it is shown that both positive and negative refraction may occur.

PACS. 41.20.Jb Electromagnetic wave propagation; radiowave propagation

1 Introduction

Research on metamaterials has so far mainly been directed at the properties of the elements [1–5] and their collective behaviour [6,7]. The principal aim is to change the effective permittivity and permeability of the material as seen by a transverse electromagnetic wave. However, similar elements may also support other types of wave, as shown by Tretyakov [8] for loaded dipoles and by Shamonina et al. [9,10] for capacitively loaded metal loops. In the latter case, the waves arise due to induced voltages caused by magnetic coupling between the elements: hence the name of magneto-inductive or MI waves. They can propagate within a band near the resonant frequency of the elements, the bandwidth being roughly proportional to the coupling coefficient. They may exist as forward and backward waves depending on the orientation of the elements. Theoretical predictions for the one-dimensional case [9] were confirmed experimentally by Wiltshire et al. both for resonant loops [11] and for 'Swiss Roll' resonators [12]. An application of MI waves in delay lines has been recently proposed by Freire et al. [13], and focusing by MI waves has been recently reported by Freire and Marques [14].

Since MI waves have been studied for only a few years it is worth putting them in context. They are not electromagnetic waves, in the sense that their dispersion characteristic is independent of the velocity of light. They resemble more closely acoustic waves in crystals [15] or plasma waves propagating along metallic nanoparticle chains [16,17], since the properties of all these waves are derived from nearest-neighbour interactions, and may be described by one-dimensional theories. MI waves could have been predicted at any time since Faraday's discovery of magnetic induction but, as it happened, their properties have only recently been investigated.

Reflection and refraction of waves traveling from one medium into another medium is also an old subject. When both media can be described by the material constants of permeability and permittivity and the input wave is an electromagnetic wave, then the solution is relatively easy. When one of the media is a periodic one then the solution may be much more complicated. For an electromagnetic wave incident upon a perfect crystal see for example the analysis of Mahan and Obermair [18]. For the one-dimensional case when an electromagnetic wave is incident upon a periodically loaded medium an elegant formula for the reflection coefficient is derived by Tretyakov [19]. The solution is valid when no higher orders are present and the interface is very simple (see Sect. 4 for what we mean by a simple interface).

When both media are periodic there is little guidance available on how to treat the reflection problem. Reflection coefficients at the junction of two acoustic lattices or two electric transmission lines, modeled by a periodic array of L-C circuits, may be found in Brillouin's book [15] in terms of characteristic impedances. These formulae are valid as long as the interface can be disregarded. A method that is general enough to treat the reflection problem, including the effect of the interface, was proposed by Syms [20] in a quite different context when investigating diode laser

[a] e-mail: r.syms@imperial.ac.uk

arrays modeled as sets of coupled waveguides. The reflection that occurs at the interface of two dissimilar sets of coupled guides is derived, by considering nearest neighbor interactions across the boundary. We shall, in the present paper, apply the same method for the 2D reflection and refraction of MI waves. There is an added interest in the solution of this set of problems since, due to the possibility of supporting both forward and backward waves, negative refraction may also take place.

The phenomenon of negative refraction has been widely investigated in the last six years ever since Smith et al. [6] and Pendry [21] rediscovered Veselago's [22] work on negative refractive index materials (which he termed Left-Handed Media). Because a negative refractive index implies the presence of backward waves, Lindell et al. [23] suggested that media exhibiting these effects be termed Backward Wave Media. Considering that backward wave structures were widely used in microwave engineering [24,25], experiments to explore negative refraction could have been proposed any time in the last six decades. As it happened, those investigations did not take place until recently, spurred by Veselago's concept of negative refractive index and Notomi's [26] realization that a backward wave structure exists in a strongly modulated Photonic Band Gap material within a certain frequency range near to the band edge. By now there is considerable experimental evidence for negative refraction both in Left-Handed Media [7,27–30] and in Photonic Band Gap (PBG) materials [31–34]. A different arrangement was proposed by Luo et al. [35], who showed that for certain orientations in a PBG material negative refraction is obtained without the existence of negative group velocity. In all the examples quoted above an electromagnetic wave was incident from vacuum upon the material that exhibited negative refraction. But electromagnetic waves are not unique in this respect. Other waves may also suffer negative refraction provided the parameters of the two media are carefully chosen. In fact, Torres and Montero de Espinosa [36] have recently designed an artificial acoustic medium that can show negative refraction. In principle it would be very simple to find negative refraction at the boundary of two acoustic media if one could freely choose the parameters. A simple condition is that at the same frequency a forward wave should propagate in medium 1, and a backward wave in medium 2 (due to the 'optical' branch).

The aim of this paper is to show how MI waves reflect and refract at the boundary of two 2D media and find the coefficients of reflection and transmission. MI waves are highly suitable for studying refraction problems because the dispersion characteristics can be easily controlled by the parameters available (the loop diameter, number of turns, value of capacitance, distance between the elements and, most importantly the orientation of the loops). It is also possible to make the arrangement biperiodic by alternating the loop diameters in an array. This structure leads to the equivalent of the 'optical' branch of acoustic waves [37]. MI waves are so versatile that at a given frequency practically any angle between the phase and group velocities can be realized. We emphasize that negative refraction is only one by-product of our investigations. It is not our aim to find the exact conditions for its existence; we shall only discuss the issue here and offer an example. To introduce the concepts we shall start in Section 2 with the 2D recurrence relationships between the currents flowing in neighbouring elements, from which the dispersion relationship, group velocity and power density vector of MI waves are derived. Section 3 is concerned with the construction of the angle of refraction, and Section 4 with the derivation of reflection and transmission coefficients. Conclusions are drawn in Section 5.

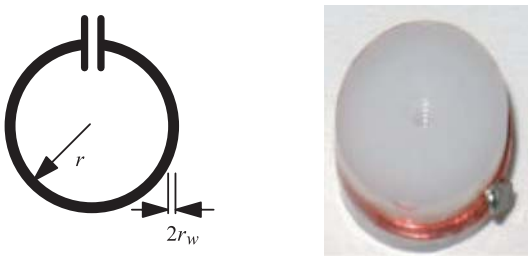

a) b)

Fig. 1. (a) Schematic representation and (b) actual realization of a capacitively loaded metallic loop. The photograph is taken from reference [10].

2 Dispersion equation, group velocity and power density

The basic element in our 2D array is the capacitively loaded metallic loop, shown schematically in Figure 1, together with an actual realization [10]. Here, r is the mean radius of the loop and r_w is the radius of the wire. We shall investigate the case when the loops are arranged in a regular rectangular lattice with the same lattice constant a in both directions. There are two configurations of interest, the planar (all elements in the same plane, Fig. 2a) and the planar-axial (all elements in the same plane in one direction but with their plane perpendicular to the axis in the other direction, Fig. 3a).

The fundamental relationship between the currents may be derived from Kirchhoff's voltage law, which requires that the total voltage round any of the loops must be zero. Taking into account only nearest neighbour interactions, the relationship may be written in the form:

$$\{j\omega L + 1/j\omega C\}I_{n,m} + j\omega M_x(I_{n+1,m} + I_{n-1,m}) + j\omega M_y(I_{n,m+1} + I_{n,m-1}) = 0 \quad (1)$$

Here $I_{n,m}$ is the current in the element $(n,\ m)$ located at the nth row and mth column, L and C are the inductance and capacitance of an element, ω is the frequency and M_x and M_y are the mutual inductances in the x and y directions respectively. Note that the loop resistance has been disregarded so we are concerned here with the loss-less case only. For the planar configuration (Fig. 2a),

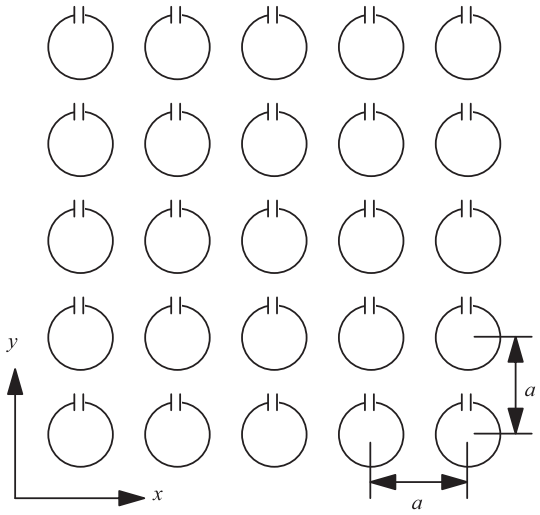

(a)

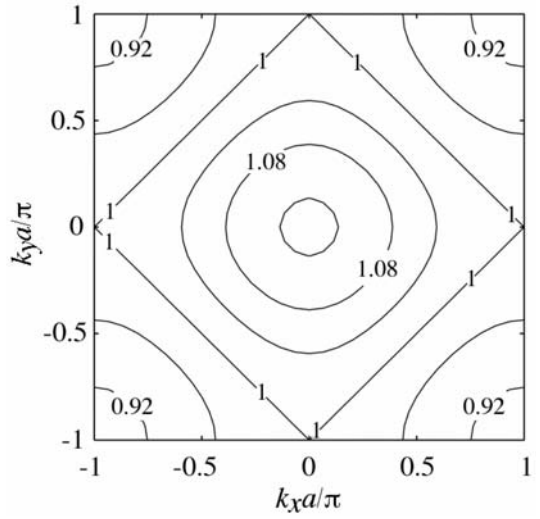

(b)

Fig. 2. Planar configuration: (a) geometry of the loops; (b) dispersion curves for $a = 2.25\ r$.

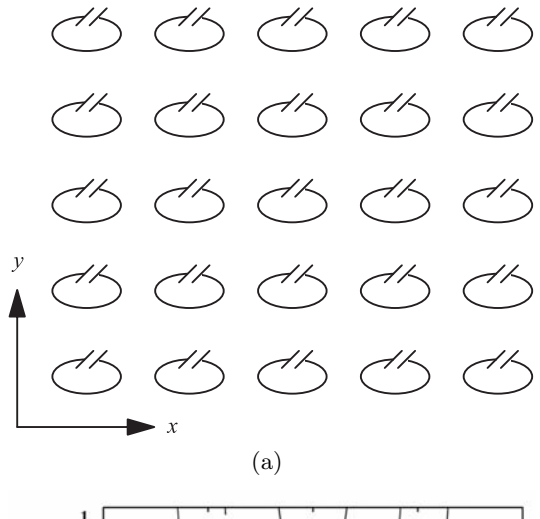

(a)

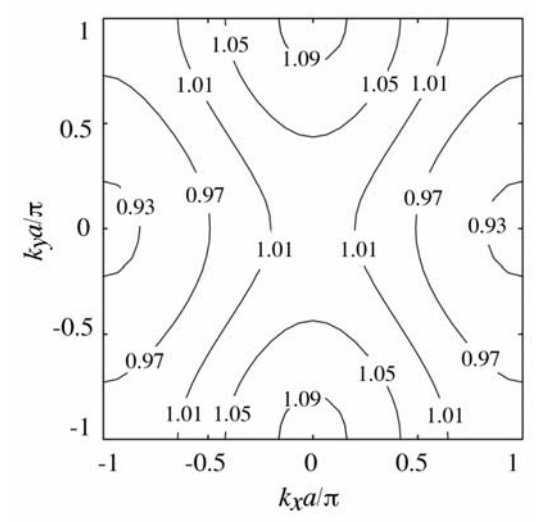

(b)

Fig. 3. Planar-axial configuration: (a) geometry of the loops; (b) dispersion curves for $a = 2.25\ r$.

$M_x = M_y$ and both values are negative due to the fact that the magnetic field generated by one element crosses the neighbouring element in the opposite direction. For the planar-axial case (Fig. 3a) M_x is still negative, but M_y is positive and under the present conditions (the element spacing being the same in both directions) its value is smaller than $|M_x|$. We assume the current in the form:

$$I_{n,m} = I_0 \exp\{-j(nk_x a + mk_y a)\}. \quad (2)$$

Here k_x and k_y are the x and y components of the propagation vector and I_0 is a constant. Substituting equation (2) into equation (1) we obtain the dispersion equation [9]:

$$\omega/\omega_0 = A^{-1/2}; A = 1 + \kappa_x \cos(k_x a) + \kappa_y \cos(k_y a). \quad (3)$$

Here κ_x and κ_y are coupling coefficients, defined as $\kappa_{x,y} = 2M_{x,y}/L$. The most useful presentation of the solution is in the form of loci of $\omega/\omega_0 =$ constant, where $\omega_0 = (LC)^{-1/2}$ is the resonant frequency of the element. These are shown in Figure 2b for the planar configuration, taking $\kappa_x = \kappa_y = -0.1$ and $a = 2.25\ r$. For the planar-axial configuration the dispersion curves shown in Figure 3b are calculated for $\kappa_x = -0.1062$, $\kappa_y = 0.0661$ and $a = 2.25\ r$. When $k_x a$ and $k_y a \ll 1$ the loci in Figure 2b tend to circles and the loci in Figure 3b to hyperbolae.

For a wave characterized by propagation constants k_x and k_y, the group velocity $\underline{v}_g$ (which defines the direction of power flow) may be obtained from equation (3) as:

$$\underline{v}_g = (a\omega^3/2\omega_0^2)\{\kappa_x \sin(k_x a)\underline{i} + \kappa_y \sin(k_y a)\underline{j}\}. \quad (4)$$

Here $\underline{i}$ and $\underline{j}$ are unit vectors in the x and y directions respectively. For the planar case, when $\kappa_x = \kappa_y$ and the arguments of both sine functions are small, the group velocity is in a direction opposite to the phase velocity – a clear case of a backward wave. The relationship is more complicated for the planar-axial configuration as will be discussed in the next section.

The group velocity vector defines the direction of power flow. It follows from the basic physics that the power density $\underline{S}$ (the power per unit length for the 2D case) is found from the product of group velocity and E_s, the stored energy per unit surface, as follows:

$$\underline{S} = (1/2)\underline{v}_g E_s. \quad (5)$$

The energy E_s stored in any of the elements is given by the sum of the energies in the inductance, the capacitance and in the mutual inductances relating to nearest neighbours. In terms of a single element (m, n), E_s is given by:

$$E_s = (1/2a^2)\left\{L|I_{n,m}|^2 + |I_{n,m}|^2/\omega^2 C + M_x I_{n,m}(I^*_{n+1,m} + I^*_{n-1,m}) + M_y I_{n,m}(I^*_{n,m+1} + I^*_{n,m-1})\right\}. \quad (6)$$

Here, * denotes the complex conjugate. Using equation (1), equation (6) may be rearranged as:

$$E_s = (L\omega_0^2/a^2\omega^2)|I_{n,m}|^2. \quad (7)$$

The power flow may then be obtained for the wave in equation (2) as:

$$\underline{S} = (\omega/2a)|I_0|^2\{M_x \sin(k_x a)\underline{i} + M_y \sin(k_y a)\underline{j}\}. \quad (8)$$

Clearly, $\underline{S}$ is independent of L and C; in fact, it only depends on the terms M_x and M_y, which give rise to propagation of energy between the elements. The power flow tends to zero when $k_x a$ and $k_y a$ are both near 0 or π, and is maximum when they tend to $\pi/2$. An expression for power may also be obtained by an entirely different method. Multiplying equation (1) by $I^*_{n,m}$, and subtracting the complex conjugate of the resulting equation yields:

$$\begin{aligned} &j\omega M_x\{(I_{n+1,m}I^*_{n,m} - I^*_{n+1,m}I_{n,m}) \\ &- (I_{n,m}I^*_{n-1,m} - I^*_{n,m}I_{n-1,m})\} \\ &+ j\omega M_y\{(I_{n,m+1}I^*_{n,m} \\ &- I^*_{n,m+1}I_{n,m}) - (I_{n,m}I^*_{n,m-1} \\ &- I^*_{n,m}I_{n,m-1})\} = 0. \end{aligned} \quad (9)$$

Equation (9) is a form of zero-divergence condition analogous to Poynting's theorem in the loss-less, steady state case. The power flow vector may then be extracted by inspection. Inserting an arbitrary scaling constant for agreement with equation (8), we obtain:

$$\underline{S} = (j\omega/4a)\{M_x(I_{n+1,m}I^*_{n,m} - I^*_{n+1,m}I_{n,m})\underline{i} + M_y(I_{n,m+1}I^*_{n,m} - I^*_{n,m+1}I_{n,m})\underline{j}\} \quad (10)$$

Equation (10) may be used when the current distribution no longer consists of a single wave.

3 Reflection and refraction at the boundary between two media

Let us assume now that we have two semi-infinite 2D media lying on each side of the line $x = 0$, that both can support MI waves, and both have the same regular rectangular lattice with a lattice constant a. We shall consider here two examples. In the first case, the elements in both media are in the planar configuration, medium 1 having the same parameters as in Figure 2b. Medium 2 differs from medium 1 by having a slightly different capacitance and consequently a slightly different resonant frequency which we shall take as $\omega_{02} = 1.03\ \omega_{01}$, as shown in Figure 4. Assuming further that $k_x a$ and $k_y a$ are small relative to unity the constant frequency curves are circles with good approximation. They are shown in Figure 5a for $\omega/\omega_{01} = 1.11$.

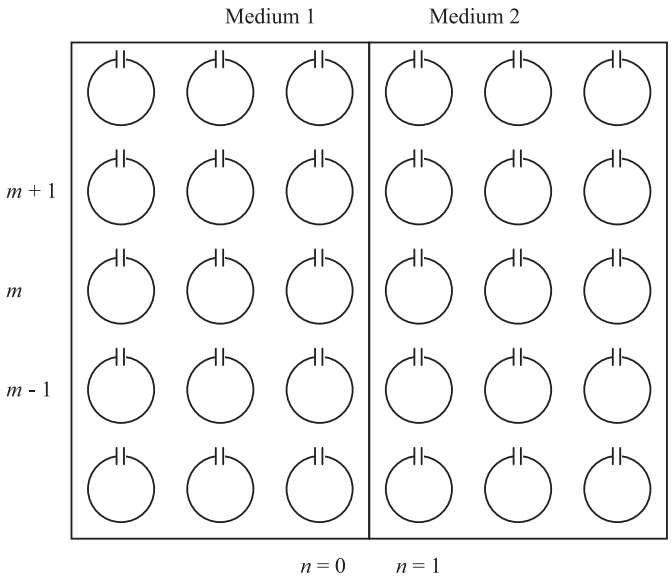

Fig. 4. Refraction at the boundary of two media. Planar configuration with $\omega_{01} \neq \omega_{02}$. The geometry of the loops.

It needs to be noted that we have here a rather unusual situation. Normally, positive refraction is due to forward waves propagating in both media. In the present case both media support backward waves. This does not lead to any complications but it means that if we want a wave incident at a positive angle (i.e. the group velocity to be in the first quarter) we have to choose k_{x1} and k_{y1} in medium 1, to be in the third quarter.

The boundary condition to be satisfied is that the tangential components of the phase velocities must match on either side of the boundary, so that $k_{y2} = k_{y1}$ and k_{x2} is given by the construction shown in Figure 5a. The corresponding group velocities, very nearly opposite to the chosen wave vectors, are shown in Figure 5b. It may be seen from Figure 5a that the construction can be performed for all possible values of k_{x1}, i.e. at that particular frequency a refracted wave exists for any incident wave.

In our next example we shall take the same planar configuration on both sides of the boundary but now the resonant frequency is assumed to be smaller in medium 2. We take $\omega_{02} = 0.97\omega_{01}$. The ratio of the radii is then reversed, as shown in Figure 6a. Using the same construction as before we find that $k_{x2} > k_{x1}$ and refraction is now pointing away from the perpendicular as may be seen in Figure 6b

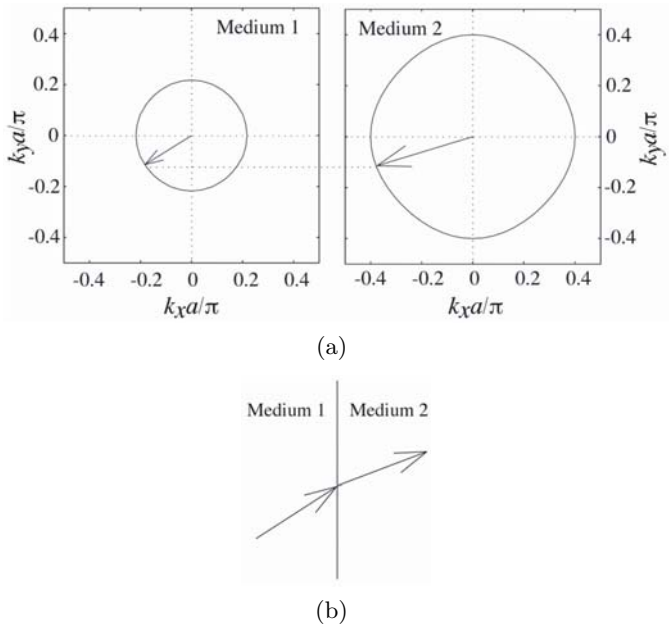

Fig. 5. Refraction at the boundary of two media. Planar configuration with ω_{02}/ω_{01}= 1.03. (a) The loci ω/ω_{01}= 1.11 and corresponding phase velocity vectors; (b) directions for the group velocity vectors, assuming $(k_{x1}a,\, k_{y1}a) = (-0.18, -0.12)$ π and $(k_{x2}a,\, k_{y2}a) = (-0.38, -0.12)\pi$.

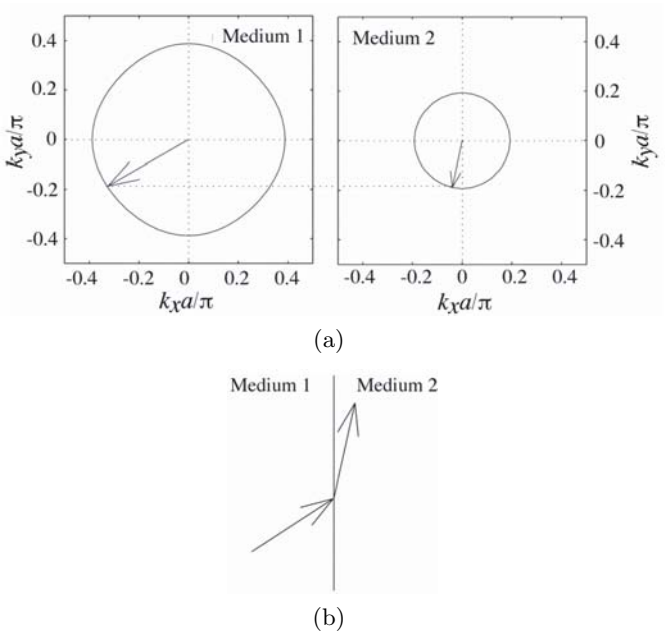

Fig. 6. Refraction at the boundary of two media. Planar configuration. ω_{02}/ω_{01}= 0.97. (a) The loci ω/ω_{01}= 1.08 and corresponding phase velocity vectors; (b) directions for the group velocity vectors, assuming $(k_{x1}a,\, k_{y1}a) = (-0.33, -0.19)$ π and $(k_{x2}a,\, k_{y2}a) = (-0.04, -0.12)\pi$.

where the corresponding group velocities are shown at the boundary of the two media. It may also be seen in Figure 6a that no refraction is possible for a range of incident angles. This is the case of total internal reflection.

In our third example we choose planar-axial configurations on both sides. All the parameters are the same but the orientation in medium 2 is at right angle to that in medium 1 as shown in Figure 7a. Note that the lattice in medium 2 is shifted by half a lattice constant relative to that in medium 1, to ensure increased magnetic coupling between the two media.

Our aim is now the same as in the previous examples: we wish to have an incident wave with group velocity in the first quarter. Let us remember that the group velocity is the gradient vector of the loci ω = constant. Hence any such locus in the second quarter of the dispersion diagram, shown in Figure 3b, would qualify. Let us choose the curve $\omega/\omega_{01} = 1.01$, plotted in Figure 7b with small arrows showing the direction of the group velocity. The relevant dispersion curve for the same value of ω/ω_{01} in medium 2 is rotated by 90 degrees and is therefore in the first quarter as shown also in Figure 7b. It may be seen that there is only a very limited range of incident wave vectors for which refraction exists. The effect could be used for switching, modulation or spatial filtering for example.

Choosing now a value of $k_y a = 0.4\pi$, and adhering again to the rule that the tangential components of phase velocity must match across the boundary, the group velocities in the two media are as shown in Figure 7c. There is clearly negative refraction in this case. Note that the angle between phase and group velocities is slightly less than 90 degrees in both media, so the waves on both sides would qualify as forward waves. In fact, we could make the angles between phase and group velocity decrease further by choosing $\omega/\omega_0 = 1$ or increase the angle (going thereby into the region where the waves on both sides are backward waves) by choosing $\omega/\omega_0 = 1.01$. This is similar to the conclusions reached by Luo et al. [35] in the sense that negative refraction may occur without the presence of backward waves, but in our case the refraction angle is a strongly varying function of the incident angle.

We could also change the angle of negative refraction in medium 2 by leaving medium 1 unchanged and rotating the orientation of the loops in medium 2, relative to medium 1, by less than 90 degrees. In addition we could considerably influence the dispersion characteristics of MI waves in medium 2 by changing the resonance frequency and the coupling coefficients. Clearly, there are many possible configurations that show negative refraction. Any combination of the four possibilities may occur: (i) both waves forward, (ii) both waves backward, (iii) incident wave in medium 1 forward, refracted wave in medium 2 backward and (iv) incident wave in medium 1 backward, refracted wave in medium 2 forward.

Previous efforts in the literature to find negative refraction were aimed at electromagnetic waves incident from free space upon a periodic medium. In our case both media are periodic. The MI wave, quite obviously, could not be incident from free space because it can exist only in certain periodic media. It needs to be noted that we have a large amount of freedom choosing the dispersion characteristics

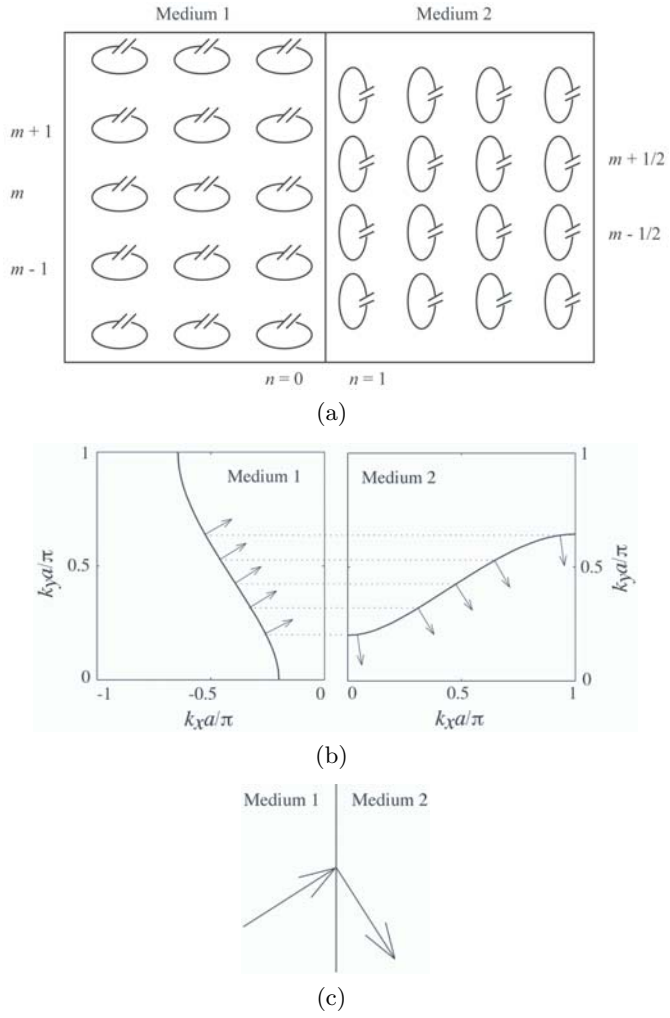

Fig. 7. Refraction at the boundary of two media. Planar-axial configuration with different orientations of the loops in medium 1 and medium 2. (a) The geometry of the loops; (b) the loci ω/ω_{01}= 1.01 and directions for group velocity vectors; (c) directions for the group velocity vectors for $(k_{x1}a, k_{y1}a) = (-0.39, -0.42)\pi$.

in both media allowing thereby a large variety of refractive angles, both positive or negative, to be realized.

4 Reflection and transmission coefficients

It is not trivial to derive the reflection and transmission coefficients in a general case when the relative positions of the elements on the two sides of the boundary are arbitrary. Our method of solution, based on that of [20], is generally applicable, but the solutions presented here will be restricted to our three examples. Examples 1 and 2 represent the simplest possible case when only the capacitances on the two sides are different, and all the coupling coefficients (not only those in the bulk media but that across the boundary as well) are identical.

Under the nearest neighbor approximation the effect of only one column on each side of the boundary needs to be considered. These two columns are numbered $n = 0$, 1 and the rows as $m - 1$, m, and $m + 1$ in Figure 4. The governing equation (1) is of course still valid. There are no new features when it is applied to elements in column -1 or column 2. But for elements in the immediate vicinity of the boundary the voltage induced in them depend not only on currents on the same side but also upon currents in elements on the other side of the boundary. The voltage induced in the element (0, m) will now depend on the current in the element (1, m) and vice versa. And of course the currents on the two sides of the boundary obey now different relationships firstly because the x-components of the propagation vector are different and secondly because there is now an additional reflected wave in medium 1 and only a single transmitted wave in medium 2. The currents can be assumed in the form:

$$\begin{aligned} I_{n,m} =& I_0\{\exp(-jnk_{x1}a) + R\exp(jnk_{x1}a)\} \\ & \times \exp(-jmk_{y1}a) \qquad n \le 0 \\ I_{n,m} =& I_0 T\exp(-jnk_{x2}a)\exp(-jmk_{y2}a) \qquad n \ge 1. \end{aligned} \quad (11)$$

Here I_0 is the amplitude of the incident wave, and R and T are the reflection and transmission coefficients respectively. Note that $k_{y1} = k_{y2}$ so that the y-variation is the same in both media. Away from the boundary, these solutions satisfy the governing equations for the two bulk media. However, at the boundary itself, we must solve the modified equations:

$$\begin{aligned} &\{j\omega L + 1/j\omega C_1\}I_{0,m} + j\omega M_x(I_{1,m} + I_{-1,m}) \\ &\quad + j\omega M_y(I_{0,m+1} + I_{0,m-1}) = 0 \\ &\{j\omega L + 1/j\omega C_2\}I_{1,m} + j\omega M_x(I_{2,m} + I_{0,m}) \\ &\quad + j\omega M_y(I_{1,m+1} + I_{1,m-1}) = 0. \end{aligned} \quad (12)$$

Here, C_1 and C_2 are the capacitances in medium 1 and medium 2, respectively. Substitution of equations (11) into equations (12) yields two simultaneous equations for R and T, which can be solved to obtain:

$$\begin{aligned} R &= \frac{-\{\exp(-jk_{x2}a) - \exp(-jk_{x1}a)\}}{\{\exp(-jk_{x2}a) - \exp(+jk_{x1}a)\}} \\ T &= \frac{\exp(-jk_{x1}a) - \exp(+jk_{x1}a)}{\{\exp(-jk_{x2}a) - \exp(+jk_{x1}a)\}}. \end{aligned} \quad (13)$$

Equation (12) implies that both coefficients depend only on the x components of the propagation vector on the two sides. When the two media are identical, i.e. $k_{x1} = k_{x2}$, the above expressions may be seen to reduce to $R = 0$ and $T = 1$ as expected. It may also be seen that $|R|^2 = 1$ when k_{x2} is purely imaginary, indicating total internal reflection.

The reflection coefficient in equation (12) agrees with equation (5.115) in Tretyakov's book [19], although the two formulae have been derived for quite different cases. Tretyakov's formula is for an incident electromagnetic wave, and is derived by ignoring the boundary. Equation (12) is for a MI wave incident from a periodic medium, and the effect of the boundary is taken exactly into account within the accuracy of the nearest neighbour interaction assumption. The reason for the agreement is

twofold; firstly waves of different kinds may obey the same relationships and secondly, more importantly, we have chosen here a simple arrangement where the coupling across the boundary is the same as in the bulk media. As a result, the boundary has no special influence. The same is not true in other cases.

As an example, we consider a case that is only slightly different, when the self-inductances are also different on either side of the boundary. As a result, the mutual inductances must also be different; we take them as M_{x1} and M_{y1} in the x- and y-directions in medium 1 and M_{x2} and M_{y2} in medium 2. Across the boundary, the mutual inductance must have a value that is different from both M_{x1} and M_{x2}; we take this as M_{x3}. The equations we must solve at the boundary are therefore:

$$\begin{aligned}&\{j\omega L_1 + 1/j\omega C_1\}I_{0,m} + j\omega M_{x3}I_{1,m} + j\omega M_{x1}I_{-1,m}\\&+j\omega M_{y1}(I_{0,m+1} + I_{0,m-1}) = 0\\&\{j\omega L_2 + 1/j\omega C_2\}I_{1,m} + j\omega M_{x2}I_{2,m} + j\omega M_{x3}I_{0,m}\\&+j\omega M_{y2}(I_{1,m+1} + I_{1,m-1}) = 0.\end{aligned} \quad (14)$$

Substituting equations (11) into equations (14) and solving for R and T, we now obtain:

$$\begin{aligned}R &= \frac{-\{M_{x3}^2\exp(-jk_{x2}a) - M_{x1}M_{x2}\exp(-jk_{x1}a)\}}{\{M_{x3}^2\exp(-jk_{x2}a) - M_{x1}M_{x2}\exp(+jk_{x1}a)\}}\\T &= \frac{M_{x1}M_{x3}\{\exp(-jk_{x1}a) - \exp(+jk_{x1}a)\}}{\{M_{x3}^2\exp(-jk_{x2}a) - M_{x1}M_{x2}\exp(+jk_{x1}a)\}}.\end{aligned} \quad (15)$$

Clearly, equation (15) is no longer identical to the simple formula derived by Tretyakov, since the coupling elements M_{x1}, M_{x2} and M_{x3} now appear; in fact, it corresponds to the solution found in [20] for coupling between dissimilar coupled waveguide arrays.

Further geometric modifications — as in our previous example 3 — generate additional departures from the simple solution. It is more difficult to derive the reflection and transmission coefficients in this case, because the elements in medium 2 are shifted relative to those in medium 1. This aspect requires the introduction of a new numbering of the rows as $m - 1/2$, $m + 1/2$, etc., as shown in Figure 7a. Kirchhoff's equations across the boundary must now take into account five, instead of four, nearest neighbours. The boundary equations are now:

$$\begin{aligned}&\{j\omega L + 1/j\omega C\}I_{0,m} + j\omega M_{x1}I_{-1,m}\\&\quad + j\omega M_{xy}(I_{1,m+1/2} - I_{1,m-1/2})\\&\quad + j\omega M_{y1}(I_{0,m+1} + I_{0,m-1}) = 0\\&\{j\omega L + 1/j\omega C\}I_{1,m-1/2} - j\omega M_{xy}(I_{0,m} - I_{0,m-1})\\&\quad + j\omega M_{x2}I_{2,m-1/2}\\&\quad + j\omega M_{y2}(I_{1,m+1/2} + I_{1,m-3/2}) = 0.\end{aligned} \quad (16)$$

Here M_{x1}, M_{y1}, M_{x2} and M_{y2} are the mutual inductances in medium 1 and 2 in the x and y directions, and M_{xy} is the mutual inductance across the boundary between the elements (0, m) and (1, m+1/2). By symmetry, the mutual inductance between elements (0, m) and $(1, m-1/2)$ is $-M_{xy}$. Substituting equations (11) into equations (14) and solving for R and T, we now obtain:

$$\begin{aligned}R &= \\&\frac{-\{4M_{xy}^2\sin^2(k_{y1}a/2)\exp(-jk_{x2}a) - M_{x1}M_{x2}\exp(-jk_{x1}a)\}}{\{4M_{xy}^2\sin^2(k_{y1}a/2)\exp(-jk_{x2}a) - M_{x1}M_{x2}\exp(+jk_{x1}a)\}}\\T &= \\&\frac{2jM_{x1}M_{xy}\sin(k_{y1}a/2)\{\exp(-jk_{x1}a) - \exp(+jk_{x1}a)\}}{\{4M_{xy}^2\sin^2(k_{y1}a/2)exp(-jk_{x2}a) - M_{x1}M_{x2}\exp(jk_{x1}a)\}}.\end{aligned} \quad (17)$$

Equation (17) now contains not only the mutual inductances M_{x1}, M_{x2}, and M_{xy}but also the y-components of the k-vectors appearing in the problem. Effectively, this is because each element $(1, m-1/2)$ receives phased contributions from elements (1, m) and (0, $m-1$) across the boundary, giving rise to a further departure from the simple solution. One clear difference is therefore that the transmission is zero when $k_{y1}a = 0$, so that total reflection occurs at normal incidence.

Finally, we consider power flow. It is, obviously, a requirement that the x component of the power density vector must be conserved across the boundary. It should therefore follow that:

$$M_{x1}\sin(k_{x1}a)\{1 - |R|^2\} = M_{x2}\sin(k_{x2}a) \quad |T|^2. \quad (18)$$

Substituting the values of R and T from the examples above, we find after some algebra that power is indeed conserved in each case.

5 Conclusions

The reflection and refraction of magnetoinductive waves propagating along discrete sets of capacitively loaded loops have been studied in the nearest-neighbor interaction approximation for the two-dimensional case. Three examples have been investigated. In the first two configurations, the loop orientations are identical in the two media, the waves propagating are backward waves and the mutual inductance across the boundary is assumed to be the same as the mutual inductances in the bulk media. It has been shown that under these conditions the refraction is positive. In the third example, when the orientations of the loops are different in the two media, it has been shown that each medium is capable of propagating both forward and backward waves and negative refraction may occur when the waves are forward on both sides.

Reflection and transmission coefficients have been derived based on the method of reference [20]. For the first two cases those coefficients have been shown to depend only on the x-components of the propagation vectors on the two sides, whereas for the more general third case the coefficients depend not only on the propagation vector but also on all the mutual inductances. The power density carried by the MI wave is determined, and it is shown that its normal component is conserved across the boundary.

The Authors gratefully acknowledge the support of EPSRC under grant GR/S67135/01 "Platform Support for 3D Electrical MEMS". E. Shamonina acknowledges financial support by the Emmy-Noether Program of the German Research Council.

References

1. J.B. Pendry, A.J. Holden, W.J. Stewart, I. Youngs, Phys. Rev. Lett. **76**, 4773 (1996)
2. J.B. Pendry, A.J. Holden, D.J. Robbins, W.J. Stewart, IEEE Trans. Micr. Theor. Tech. **47**, 2075 (1999)
3. P. Gay-Balmaz, O.J.F. Martin, Appl. Phys. Lett. **81**, 939 (2002)
4. R. Marques, F. Mesa, J. Martel, F. Medina, IEEE Trans. Antennas Propag. **51**, 2572 (2003)
5. M. Shamonin, E. Shamonina, V. Kalinin, L. Solymar, J. Appl. Phys. **95**, 3778 (2004)
6. D.R. Smith, W.J. Padilla, D.C. Vier, S.C. Nemat-Nasser, S. Schultz , Phys. Rev. Lett. **84**, 4184 (2000)
7. R.A. Shelby, D.R. Smith, S. Schultz, Science **292**, 77 (2001)
8. S.A. Tretyakov, A.J. Viitanen, Elect. Engng. **82**, 353 (2000)
9. E. Shamonina, V.A. Kalinin, K.H. Ringhofer, L. Solymar, Elect. Lett. **38**, 371 (2002)
10. E. Shamonina, V.A. Kalinin, K.H. Ringhofer, L. Solymar, J. Appl. Phys. **92**, 6252 (2002)
11. M.C.K. Wiltshire, E. Shamonina, I.R. Young, L. Solymar, Elect. Lett. **39**, 215 (2003)
12. M.C.K. Wiltshire, E. Shamonina, I.R. Young, L. Solymar, J. Appl. Phys. **95**, 4488 (2004)
13. M.J. Freire, R. Marques, F. Medina, M.A.G. Laso, F. Martin , Appl. Phys. Lett. **85**, 4439 (2004)
14. M.J. Freire, R. Marques, presented at the *Latsis Conference on Negative Refraction*, Lausanne, February 28–March 2 (2005)
15. L. Brillouin, *Wave Propagation in Periodic Structures* (McGraw-Hill Book Co. Ltd, New York, 1946)
16. M. Quinten, A. Leitner , J.R. Krenn, F.R. Aussenegg, Opt. Letts. **23**, 1331 (1998)
17. W.H. Weber, G.W. Ford, Phys. Rev. B **70**, 125429 (2004)
18. G.D. Mahan, G. Obermair, Phys. Rev. **183**, 834 (1969)
19. S. Tretyakov, *Analytical Modeling in Applied Electromagnetics* (Artech House, Boston, 2000)
20. R.R.A. Syms, IEEE J. Quant. Elect. **QE-23**, 525 (1987)
21. J.B. Pendry, Phys. Rev. Lett. **85**, 3966 (2000)
22. V.S. Veselago, Sov. Phys. Usp. Fiz Nauk **92**, 517 (1967)
23. I.V. Lindell, S.A. Tretyakov, K.I. Nikoskinen, S. Ilvonen, Micr. Opt. Tech. Lett. **31**, 129 (2001)
24. P.E. Mayes, G.A. Deschamps, W.T. Patton, Proc. IRE **49**, 962 (1961)
25. R.G.E. Hutter, *Beam and Wave Electronics in Microwave Tubes* (Van Nostrand, Princeton, NJ, 1964)
26. M. Notomi, Phys. Rev. B **62**, 10696 (2000)
27. C.G. Parazzoli, R.B. Greegor, K. Li, B.E.C. Koltenbah, Tanielian M., Phys. Rev. Lett. **90**, 107401 (2003)
28. A.A. Houck, J.B. Brock, I.L. Chuang, Phys. Rev. Lett. **90**, 137401 (2003)
29. E. Ozbay, K. Aydin, E. Cubukcu, M. Bayindir, IEEE Trans. Antennas Propag. **51**, 2592 (2003)
30. L. Ran, J. Huangfu, H. Chen, Y. Li, X. Zhang, K. Chen, J.A. Kong, Phys. Rev. B **70**, 073102 (2004)
31. H. Kosaka, T. Kawashima, A. Tomita, M. Notomi, T. Tamamura, T. Sato, S. Kawakami , Phys. Rev. B **58**, 10096 (1998)
32. E. Cubukcu, K. Aydin, E. Ozbay, S. Foteinopolou, C.M. Soukoulis, Phys. Rev. Lett. **91**, 207401 (2003)
33. S. Foteinopoulou, C.M. Soukoulis, Phys. Rev. B **67**, 235107 (2003)
34. P.V. Parimi, W.T. Lu, P. Vodo, J. Sokoloff, J.S. Derov, S. Sridhar, Phys. Rev. Lett. **92**, 127401 (2004)
35. C. Luo, S.G. Johnson, J.D. Joannopoulos, J.B. Pendry, Phys. Rev. B **65**, 201104 (2002)
36. M. Torres, F.R.M. de Espinosa, Ultrasonics **42**, 787 (2004)
37. O. Sydoruk, O. Zhuromskyy, E. Shamonina, presented at the *Latsis Conference on Negative Refraction*, Lausanne, February 28–March 2 (2005)